Polymer-Based n-Type Yarn for Organic Thermoelectric Textiles

ADVANCED ELECTRONIC MATERIALS
Open Access
www.advelectronicmat.de

Polymer-Based n-Type Yarn for Organic Thermoelectric Textiles

*Sozan Darabi, Chi-Yuan Yang, Zerui Li, Jun-Da Huang, Michael Hummel, Herbert Sixta, Simone Fabiano, and Christian Müller**

A conjugated-polymer-based n-type yarn for thermoelectric textiles is presented. Thermoelectric textile devices are intriguing power sources for wearable electronic devices. The use of yarns comprising conjugated polymers is desirable because of their potentially superior mechanical properties compared to other thermoelectric materials. While several examples of p-type conducting yarns exist, there is a lack of polymer-based n-type yarns. Here, a regenerated cellulose yarn is spray-coated with an n-type conducting-polymer-based ink composed of poly(benzimidazobenzophenanthroline) (BBL) and poly(ethyleneimine) (PEI). The n-type yarns display a bulk electrical conductivity of 8×10^{-3} S cm^{-1} and Seebeck coefficient of −79 µV K^{-1}. A promising level of air-stability for at least 13 days can be achieved by applying an additional thermoplastic elastomer coating. A prototype in-plane thermoelectric textile, produced with the developed n-type yarns and p-type yarns, composed of poly(3,4-ethylenedioxythiophene):poly(styrenesulfonate) (PEDOT:PSS)-coated regenerated cellulose, displays a stable device performance in air for at least 4 days with an open-circuit voltage per temperature difference of 1 mV °C^{-1}. Evidently, polymer-based n-type yarns are a viable component for the construction of thermoelectric textile devices.

1. Introduction

Textiles are a versatile platform for wearable electronics because they readily permit the placement of a multitude of devices in close proximity to the user.[1,2] A wide range of electronic textile (e-textile) devices have been demonstrated, ranging from sensors for health monitoring[3] to keyboards,[4] displays[5] and wearable antennas for communication.[6] E-textiles can be powered by equipping them with the ability to harvest energy on the spot via the integration of solar cells,[7,8] or piezoelectric,[9,10] triboelectric,[11] and thermoelectric devices.[12–14] Thermoelectric textile devices are intriguing because they would allow to exploit ubiquitous local temperature gradients, for example, the difference in temperature between skin and the surroundings, separated by a garment.

Thermoelectric devices convert heat to electricity based on the Seebeck effect. When a thermoelectric material experiences a temperature gradient ΔT a potential difference ΔV is generated across the material according to $\Delta V = -\alpha \Delta T$, where α is the material-specific Seebeck coefficient which is positive for p-type and negative for n-type materials. Thermoelectric devices are composed of thermocouples, each one of them consisting of one n-type and one p-type leg, which are connected electrically in series but thermally in parallel so that the voltage generated by the two legs is additive. Each thermocouple only generates a small voltage, which is insufficient to power an electronic device, and thus a large number of these elements must be integrated. The open-circuit voltage V_{oc} of a thermoelectric device is given by:

$$V_{oc} = N_{element}\left(\alpha_p - \alpha_n\right)\Delta T \quad (1)$$

S. Darabi, Z. Li, C. Müller
Department of Chemistry and Chemical Engineering
Chalmers University of Technology
Göteborg 412 96, Sweden
E-mail: christian.muller@chalmers.se

S. Darabi, C. Müller
Wallenberg Wood Science Center
Chalmers University of Technology
Göteborg 412 96, Sweden

The ORCID identification number(s) for the author(s) of this article can be found under https://doi.org/10.1002/aelm.202201235.

DOI: 10.1002/aelm.202201235

C.-Y. Yang, J.-D. Huang, S. Fabiano
Laboratory of Organic Electronics
Department of Science and Technology
Linköping University
Norrköping 60174, Sweden

C.-Y. Yang, S. Fabiano
n-Ink AB
Norrköping 60174, Sweden

Z. Li
College of Electrical Engineering
Sichuan University
Chengdu 610065, China

M. Hummel, H. Sixta
Department of Bioproducts and Biosystems
Aalto University
Espoo 02150, Finland

S. Fabiano
Wallenberg Wood Science Center
Linköping University
Norrköping 60174, Sweden

Table 1. Overview of previously reported n-type yarns/fibers and the electrical conductivity σ and Seebeck coefficient α of these materials.

	Conducting material	Substrate yarn/fiber	Dopant	Manufacturing method	α [μV K^{-1}]	σ [S cm^{-1}]	Ref.
Inorganic materials	Bi_2Te_3	PAN[a]		Electrospinning/ sputtering/twisting	−176	8	[19]
	Bi_2Se_3			Thermal drawing	−92	763	[31]
Carbon allotropes	PCBM[b]	cotton		Dip-coating	−283	1×10^{-2}	[12]
	CNT[c]		PEI[d]	Direct spinning	−56	7850	[25]
	CNT		PEI/$NaBH_4$	–	−58	871	[28]
	CNT		PEI	–	−69	1408	[29]
	CNT		Oleamine	Electrospray coating	−64	≈780	[13]
	CNT:PEG[e]		[BMIM]PF_6[f]	Wet-spinning	−49	≈175	[24]
	SWCNT[g]: PVA[h]:PEI			Gel extrusion	−48	7×10^{-3}	[32]
	SWCNT: PVDF[i]		PEI	Wet-spinning	−38	1550	[33]
	MWCNT[j]: PVP[k]	PET		Dip-coating	−14	1	[30]
	Graphene: PEDOT:PSS[n]		PEIE[l]	Hydrothermal process	−4.2	11	[21]
	Graphene		PEIE	Chemical reduction	−16	10	[22]
Polymers	BBL:PEI	cellulose		Spray-coating	−79	8×10^{-3}	This work

[a]PAN = polyacrylonitrile; [b]PCBM = [6,6]-phenyl-C_{61}-butyric acid methyl ester; [c]CNT = carbon nanotubes; [d]PEI = polyethylenimine; [e]PEG = polyethylene glycol; [f]BMIM]PF_6 = 1-butyl-3-methylimidazolium hexafluorophosphate; [g]SWCNT = single-walled carbon nanotubes; [h]PVA = poly(vinyl alcohol); [i]PVDF = polyvinylidene fluoride; [j]MWCNT = multiwalled carbon nanotubes; [k]PVP = poly(vinylpyrrolidone); [l]PEIE = polyethyleneimine ethoxylate; [n]PEDOT:PSS = poly(3,4-ethylenedioxythiophene):poly(styrenesulfonate).

where $N_{element}$ is the number of thermocouples and α_p and α_n are the Seebeck coefficients of the p- and n-type leg, respectively.

Textile manufacturing processes are readily suitable for creating the complex patterns comprising a multitude of thermocouples that make up thermoelectric devices. For example, thermoelectric devices have been printed[15–17] or coated[18] onto an existing fabric or they have been incorporated into a textile layer through weaving,[19] knitting,[19] or stitching of conducting fibers.[12] For the latter approach, which enables the creation of textile devices from the bottom-up, electrically conducting fibers and yarns are needed. Several methods can be used to produce conducting yarns such as coating or dyeing of an existing yarn and solution- or melt spinning of a conducting material into fibers, which can subsequently be twisted into a yarn.[20]

A number of different materials have been used to produce p-type yarns, including inorganic materials,[19] graphene,[21,22] carbon nanotubes,[23–25] and conducting polymers.[12,26,27] With regard to n-type yarns, however, there are only studies that employ Bi_2Te_3,[19] fullerenes,[12] graphene,[21,22] or carbon nanotubes[24,28] (**Table 1**). As a result, promising thermoelectric textile designs have been realized with, e.g., carbon nanotube-based p- and n-type yarns.[13,24,29] Instead, n-type conducting polymers have not yet been reported for the fabrication of conducting yarns, likely due to their insufficient air stability. The lack of polymer-based n-type yarns currently limits the type of architectures that can be realized since conducting polymers tend to offer advantages in terms of cost-effective processing from solution as well as a high degree of mechanical flexibility. Polymer-based textile thermoelectric devices that have been reported consist of p-type yarns that are either combined with carbon nanotube-based n-type yarns,[30] or a conducting yarn such as silver-plated yarns with a very low Seebeck coefficient of 0.3 μV K^{-1}.[14] Due to health and environmental concerns associated with the use of carbon nanomaterials it would be of interest to develop polymer-based n-type yarns.

Here, we report the fabrication of polymer-based n-type yarns based on regenerated cellulose yarns, which were chosen as a substrate material because they offer sustainable production processes from a variety of feedstocks.[34,35] As the conducting material poly(benzimidazobenzophenanthroline) (BBL) was selected, which was recently found to yield an electrical conductivity of up to $\sigma = 8$ S cm^{-1} when processed together with poly(ethyleneimine) (PEI) from ethanol.[36] Regenerated cellulose yarns were spray-coated with an ethanol-based BBL:PEI ink resulting in n-type yarns with a bulk electrical conductivity of $\sigma_b = 8 \times 10^{-3}$ S cm^{-1} (relative to the cross-sectional area of the entire coated cellulose yarn) and promising degree of air-stability. The ambient stability was further improved by coating with an insulating thermoplastic elastomer layer, which facilitated the fabrication of thermoelectric textile devices by stitching the passivated BBL:PEI n-type yarns onto a wool fabric.

2. Results and Discussion

In a first set of experiments, we compared dip-coating and spray-coating of regenerated cellulose yarns with an ethanol-based BBL:PEI ink (1:1 weight ratio; see **Figure 1**a for chemical structures). Dip-coating involved immersing the yarn in the ink four times while spray-coating was performed with a spray gun (Figure 1b), coating approximately 1 cm-long segments of the yarn at a time (see Experimental Section for details). We did not dry the yarns subsequent to the coating step because

ADVANCED ELECTRONIC MATERIALS
Open Access
www.advelectronicmat.de

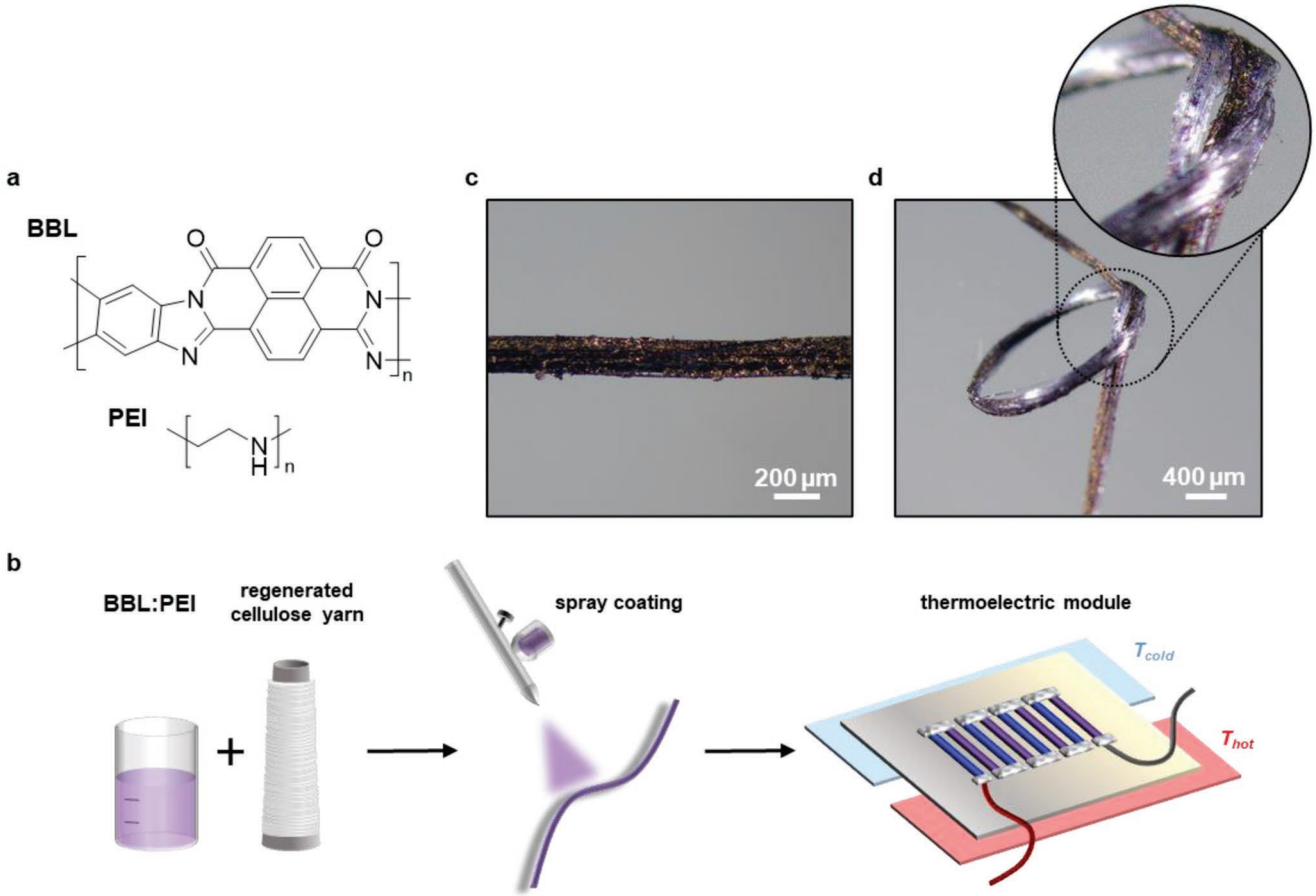

Figure 1. a) Chemical structures of poly(benzimidazobenzophenanthroline) (BBL) and poly(ethyleneimine) (PEI). b) Schematic of the preparation of electrically conducting n-type yarn through spray coating and integration of the yarn into a thermoelectric device. c,d) Optical microscopy images of the surface of a representative BBL:PEI coated cellulose yarn and the same yarn forming a loose knot.

ethanol readily evaporates. However, we thermally treated the yarns later on under an inert atmosphere (140 °C for 2 h under nitrogen; see Experimental Section for details) since polaron formation within BBL:PEI is thermally activated.[36] The n-type electrical conductivity of the BBL:PEI mixture stems from a thermally activated electron transfer from the amine-based PEI to the conjugated BBL polymer backbone. The positive charges on PEI balance the negatively charged polarons on BBL, yielding an n-doped all-polymer blend.

The quality of the applied BBL:PEI coatings from the two processes were compared by measuring the electrical resistance of the coated yarns (see Figure S1a–c, Supporting Information, for images of the samples). Dip-coated yarns featured intermittent sections with a high resistivity, indicating an inhomogeneous coating (Figure S1d, Supporting Information). In contrast, spray-coated yarns were electrically conducting along their entire length, and therefore we chose to focus on the latter type of yarn throughout the remainder of this study.

Optical and scanning electron microscopy (SEM) were used to assess the quality of the BBL:PEI coating of spray-coated yarns in more detail. Optical micrographs indicate that the polymers cover the entire yarn and do not detach upon bending (Figure 1c,d and Figure S2, Supporting Information). The surface of the here used regenerated cellulose yarns can be anticipated to predominately feature hydroxy groups, which may hydrogen-bond to the secondary amines of PEI, resulting in good adhesion between BBL:PEI and the cellulose yarn substrate. SEM images of the yarn surface and cross-section reveal a discontinuous outer coating that surrounds the yarn (**Figure 2**a–c). It appears that the conducting material, i.e., BBL:PEI, is present on the surface of some of the individual filaments as indicated by the lack of charging artifacts (Figure 2d). However, the coverage of individual yarns is likely irregular since charging artifacts also appear in SEM images recorded along the long-axis of the yarn (Figure 2a,b).

We investigated the electrical properties of spray-coated yarns by measuring their bulk electrical conductivity in two-point configuration according to:

$$\sigma_b = R^{-1} \times \frac{L}{A} \tag{2}$$

where L is the length of the measured yarn segment, A the total cross-sectional area of the yarn (calculated using the yarn diameter, which includes the insulating cellulose material as well as voids in between filaments), and R the measured resistance (see Experimental Section for details). We obtained a value of about $\sigma_b = (8 \pm 2) \times 10^{-3}$ S cm^{-1} for the here studied n-type

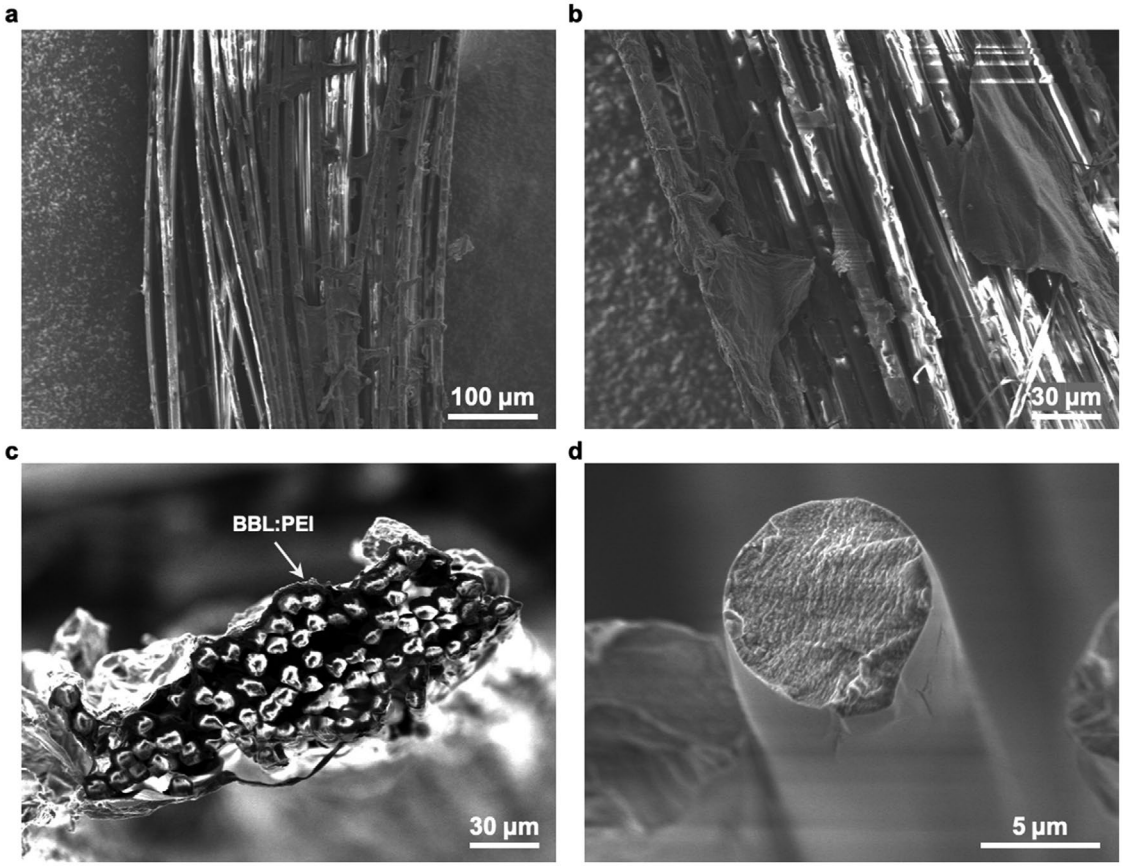

Figure 2. a–d) Scanning electron microscopy (SEM) images of the surface of a BBL:PEI coated yarn (a,b), the cross-section of a BBL:PEI-coated yarn (c), and an individual filament (d).

yarns. The linear density of neat yarns was 9.5 tex while the BBL:PEI coated yarn had a linear density of 9.8 tex (measured by weighing sections of the yarns), which indicates that ≈3 wt% of the coated yarn consisted of BBL:PEI. We thus estimate an effective conductivity for the BBL:PEI coating of 0.6 S cm^{-1} (assuming a density of 1 g cm^{-3}) by comparing the cross-sectional area of the yarn to the area of the BBL:PEI coating. The conductivity of the BBL:PEI coating is somewhat lower than the value of $\sigma = (3.1 \pm 0.1)$ S cm^{-1} measured for a reference BBL:PEI layer spray-coated onto a glass substrate. We argue that not every part of the BBL:PEI coating within the prepared yarn is continuous, thus reducing the overall electrical conductivity. Hence, the thermoelectric properties of the prepared n-type yarns could likely be improved by increasing the quality of the BBL:PEI coating. We also determined the Seebeck coefficient of as-prepared BBL:PEI coated yarns and obtained a value of $\alpha_n = -79$ µV K^{-1}, which is similar to a value of (-115 ± 9) µV K^{-1} measured for an as-prepared and annealed reference BBL:PEI film (power factor $\alpha^2\sigma = 0.4$ µW m^{-1} K^{-2} for the yarn coating and 4 µW m^{-1} K^{-2} for the reference film).

We evaluated the electrical stability of yarns stored at ambient conditions by repeatedly measuring the electrical resistance of coated yarns over the course of 2 weeks. The electrical resistance of BBL:PEI coated yarn had increased about 10 to 60 times after 13 days (**Figure 3**a). The Seebeck coefficient also varied during a repeated measurement period of 12 days at ambient conditions and increased in absolute value from –79 to –213 µV K^{-1}, indicating that the material became less doped (Figure S3, Supporting Information). Therefore, we applied an insulating barrier layer composed of the elastomer polystyrene-*b*-polyisoprene-*b*-polystyrene (SIS) (Figure 3b), leaving the yarn ends uncoated to facilitate points for electrical contact. The addition of a SIS layer led to an eightfold decrease of the initial conductivity of the yarn to 0.001 S cm^{-1}, which we assign to air exposure during the SIS coating step. The initial resistance of the 4 to 7 cm-long sections of the n-type yarns only increased five times after 13 days at ambient conditions, indicating improved ambient electrical stability (Figure 3a). We attribute the remaining change in electrical resistance to the unprotected yarn ends. BBL:PEI coated yarn stored under inert conditions displayed a ≈5 times increase in resistance after 14 days (Figure S4, Supporting Information), confirming that the here studied n-type conductor is fairly stable once protected from air.

The resilience of the n-type yarn toward deformation was investigated by performing bending tests. The yarn was bent 1000 times (bending radius = 4.2 mm) (**Figure 4**a) and the electrical resistance was measured after every 100 bending cycles using a 2-point configuration. The electrical resistance of the BBL:PEI coated yarn increased by about 20% irrespective of the presence of the additional SIS coating (Figure 4b), which suggests that the here studied materials feature a promising degree of robustness that facilitates simple textile manufacturing

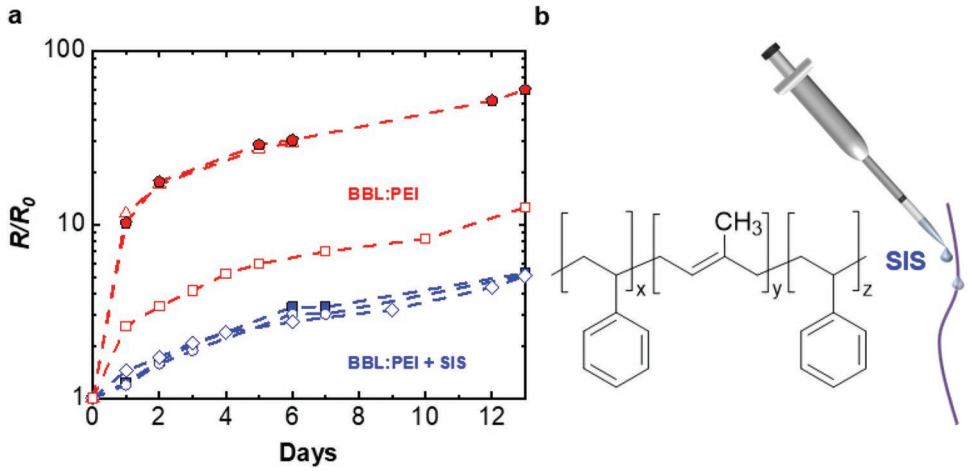

Figure 3. a) Electrical stability of BBL:PEI coated yarns stored at ambient conditions without (red) or with a SIS layer (blue) expressed as the ratio of electrical resistance R divided by the initial resistance R_0. The various symbols indicate different samples. R_0/L = 4.1, 8.8, and 10.5 MΩ cm^{-1} for the SIS coated yarns, dried for 24 h at ambient conditions before electrical characterization; R_0/L = 1.7, 1.1, and 4.2 MΩ cm^{-1} for as-prepared BBL:PEI yarns. b) Chemical structure of SIS and schematic of the process used to coat the conducting BBL:PEI yarn with a protective SIS layer.

methods such as stitching. Tensile deformation of BBL:PEI spray-coated yarn revealed a Young's modulus of (3.3 ± 0.5) GPa and strain at break of (5.1 ± 0.9)% (Figure S5, Supporting Information).

An in-plane textile thermoelectric device was fabricated by stitching yarns onto a felted wool fabric to illustrate that the BBL:PEI n-type yarn can be used for e-textile applications. The device fabrication and characterization were done at ambient conditions. The device consisted of four thermocouples (**Figure 5**a), each one comprising one n-type leg made with three BBL:PEI/SIS coated cellulose yarns with σ_n = 0.001 S cm^{-1} (value from 7 cm yarn section dried at ambient conditions post SIS coating, which differs from the yarn used in the device) and α_n = –272 μV K^{-1} (see Figure S6, Supporting Information, the change is attributed to air exposure during SIS coating and device fabrication) and one p-type leg made with two PEDOT:PSS coated cellulose yarns with σ_p = 33 S cm^{-1} and α_p = 14 μV K^{-1} (Figure S7, Supporting Information), which we have described previously.[37] The device had an internal resistance of R_{in} = 180 MΩ.

The performance of the device was assessed by placing the wool felt with one end on a hot plate while the other end was kept at ambient temperature (Figure 5b,c). The open-circuit voltage V_{oc} increased linearly with the temperature difference between the hot and cold side of the device $\Delta T = T_{hot} - T_{cold}$ with a slope of $V_{oc}/\Delta T$ = 1.0 mV °C^{-1}. The device consisted of four n–p thermocouples and thus the generated voltage scales according to:

$$V_{oc} / \Delta T = 4 \times (\alpha_p - \alpha_n) \quad (3)$$

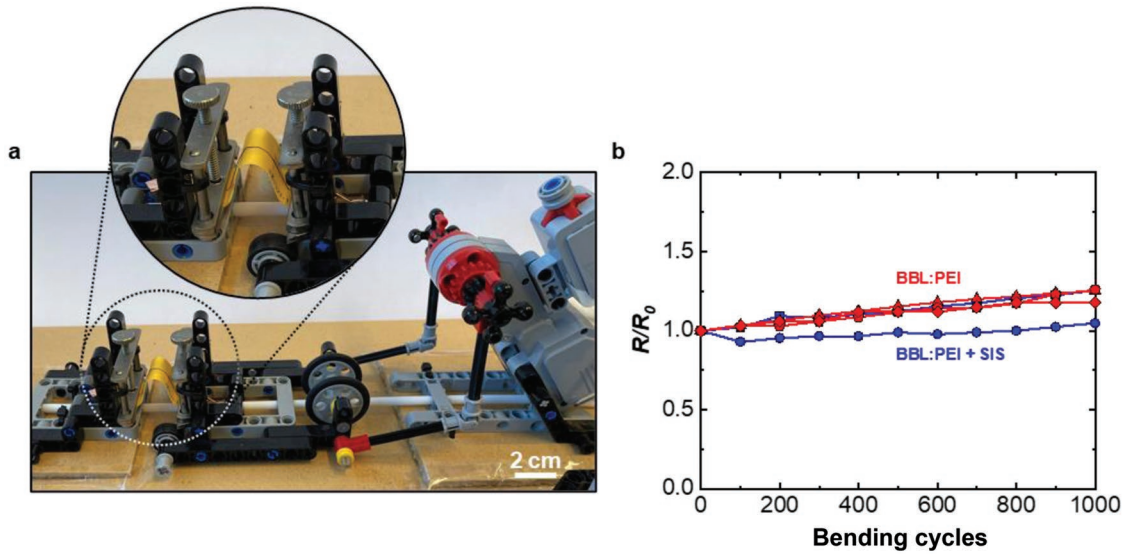

Figure 4. a) Photograph of the custom-built LEGO device used for bending tests with a mounted yarn sample. b) Electrical resistance R divided by the initial resistance R_0 measured after every 100 cycles during a total of 1000 bending cycles of BBL:PEI coated yarn (red) and BBL:PEI/SIS coated yarn (blue). The various symbols indicate different samples.

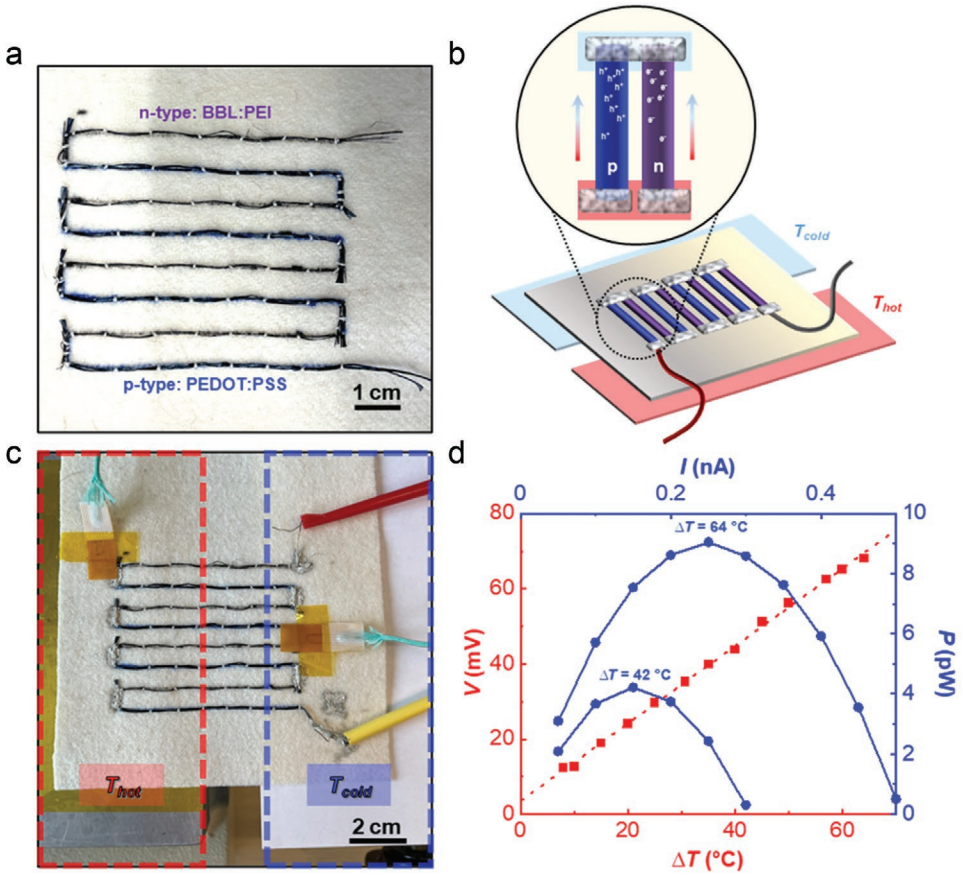

Figure 5. a) An in-plane thermoelectric textile generator stitched onto a felted wool fabric using BBL:PEI/SIS coated cellulose yarn (three yarns per n-type leg) and a PEDOT:PSS coated cellulose yarn (two yarns per p-type leg) that together form four n/p thermocouples. b) Schematic showing a close-up of a single thermocouple with the blue yarn representing the p-type PEDOT:PSS coated yarn while the purple yarn represents the n-type BBL:PEI/SIS coated yarn. The light blue area illustrates the heat sink (cold side) while the red area represents the heat source (hot side). c) The thermoelectric textile generator with the four n/p thermocouples electrically connected with stretchable silver paint and placed onto a heating source at temperature T_{not} (red) and a cold side that was kept at ambient temperature T_{cold} (blue). d) The recorded open-circuit voltage V_{oc} measured for different temperature gradients $\Delta T = T_{hot} - T_{cold}$ (red) with the output power P as a function of load current I at $\Delta T = 42$ °C or 64 °C (blue).

which yields a value of $V_{oc}/\Delta T = 1.1$ mV °C^{-1}, in good agreement with the measured value. We measured a $V_{oc} = 68$ mV for $\Delta T = 64$ °C and determined the power output for a series of load currents (Figure 5d), which yielded a maximum power output of $P_{max} = 9$ pW, in reasonable agreement with a value of 6.4 pW, predicted by using the measured values for V_{oc} and R_{in}:

$$P_{max} = \frac{V_{oc}^2}{4R_{in}} \quad (4)$$

We assign the differences in measured and predicted values to the variation in Seebeck coefficient of BBL:PEI coated yarns upon ageing (see Figure S3, Supporting Information). The performance of the thermoelectric textile device was monitored over the course of several days. Characterization was done at ambient conditions, but the device was stored in a glovebox between measurements. After 4 days the $V_{oc}/\Delta T$ had changed from 1.0 to 1.1 mV °C^{-1} and the maximum power output had decreased from 4.2 to 3.5 pW at $\Delta T = 42$ °C (Figure S8, Supporting Information), confirming that the BBL:PEI coating of the here studied n-type yarn displays improved air-stability compared with many other polymer-based n-type conductors. In addition, the textile thermoelectric device was subjected to repeated bending (6 months after device fabrication; the device was stored in a glove box) during which the Seebeck coefficient of one if its n-type legs was monitored. The initial value of $\alpha_n = -380$ μV K^{-1} changed to −319 μV K^{-1} after 400 bending cycles (Figures S9 and S10, Supporting Information; the device was exposed to air for 8 h).

3. Conclusions

Spray coating of a regenerated cellulose yarn with BBL:PEI ink resulted in an n-type yarn with robust mechanical properties. The n-type yarn displayed an electrical conductivity of $\sigma = (8 \pm 2) \times 10^{-3}$ S cm^{-1} and a Seebeck coefficient of $\alpha = -79$ μV K^{-1}. Coating of the BBL:PEI coated yarn with an additional insulating barrier layer composed of the elastomer SIS allowed to significantly improve the electrical stability of the n-type yarn at ambient conditions. The utility of the n-type yarn was illustrated by the fabrication of an in-plane thermoelectric

textile device with a stable performance for at least 4 days, with an open-circuit voltage per temperature difference of about 1 mV °C^{-1}. We conclude that the use of polymer-based n-type yarns has potential for the realization of robust and stable thermoelectric textile devices. It can be anticipated that the here presented results will stimulate further studies that ultimately lead to highly conducting polymer-based n-type yarns.

4. Experimental Section

Materials: Ioncell-F yarn and the BBL:PEI ink were prepared according to previously reported procedures.[36,38] Polystyrene-*b*-polyisoprene-*b*-polystyrene (SIS) (styrene 22 wt%) was obtained from Sigma–Aldrich, toluene and ethylene glycol from Fisher Scientific, dimethyl sulfoxide (DMSO) from VWR, and PEDOT:PSS aqueous dispersion from Heraeus (1.1–1.3 wt% solid content; Clevios PH1000). Silver paints for electrical characterization and textile device fabrication (PE874) were purchased from Agar Scientific and DuPont, respectively.

Yarn Coating: PEDOT:PSS coated yarns were prepared according to a previously published procedure.[37] To fabricate n-type yarns, the regenerated cellulose yarn was fastened on a spool while BBL:PEI ink (1 g L^{-1}), dispersed in ethanol, was repeatedly spray-coated onto the yarns at ambient conditions using a standard HD-130 airbrush (0.3 mm) with 2 bars of atomization air pressure, followed by annealing inside a nitrogen-filled glovebox by placing the yarn on a heating plate at 140 °C for 2 h. BBL:PEI thin films were also produced through spray-coating. The annealed BBL:PEI coated yarn was coated with SIS in toluene (100 g L^{-1}) by pipetting droplets onto the yarn, except for the yarn ends, at ambient conditions. The SIS layer was dried for 24 h at ambient conditions before electrical characterization or in a glovebox before textile device fabrication.

Electrical Characterization: The electrical resistance of 0.8 cm-long sections of the yarns, placed on a glass slide and contacted with silver paint, was determined in 2-point configuration using a Keithley 2400 source measure unit. A custom-built LEGO device was used to perform repeated bending of the yarns (≈7 cm-long segments), attached to a paper frame and contacted with silver paint and copper tape, with a bending radius of ≈4.2 mm. The Seebeck coefficient of 5 mm-long yarn sections, contacted with silver paint on either end, was measured at ambient conditions with a SB1000 instrument and a K2000 temperature controller from MMR Technologies. A constantan wire was used as the reference.

The BBL:PEI thin films were characterized while inside the glovebox and the Seebeck coefficient as well as the electrical conductivity were measured according to previously reported procedures.[36]

Optical Microscopy: The diameter of the yarns was determined with a Carl Zeiss A1 optical microscope in bright field transmission mode and images of the knotted yarn were recorded with a Carl Zeiss Stemi 508 stereo microscope.

Scanning Electron Microscopy: Fracture surfaces were prepared by cutting yarns immersed in liquid nitrogen. SEM images were recorded with a JSM-7800F prime instrument equipped with a secondary electron detector at an acceleration voltage of 3 kV. The BBL:PEI coated yarns were annealed, as previously explained, and later cut with scissors while immersed in liquid nitrogen. Samples were not sputtered.

Tensile Deformation: Stress–strain curves were recorded with a Q800 dynamic mechanical analyzer (DMA) from TA instruments. Yarn sections were mounted by first fixating either end with glue (Loctite Super Glue Precision) between two pieces of paper to prevent the yarn from slipping, which were then held in place by a pair of film tension clamps. A pre-load force of 1 mN was applied and a ramp force rate of 10 to 18 N min^{-1} was used.

Textile Device Fabrication and Characterization: A textile thermoelectric generator was produced by stitching p- and n-type yarns onto a felted wool fabric from Harry Hedgren AB (Wadmal, 3.2 g dm^{-2}, ≈1 mm thick). Each n- and p-type leg consisted of three and two yarns, respectively, and stretchable silver paint (PE874 from DuPont), cured at 100 °C for 20 min, was used to improve the electrical connection between legs. The textile device was placed with one side on a hot plate (HP60, Torrey Pines Scientific Inc.) and the other side on a stage that was kept at room temperature. K-type thermocouples were attached to both sides to record the temperature difference using a cDAW 9174 instrument from National Instruments with an internal temperature reference. The hot side of the device was kept in place with a weight of about 1 kg. The open-circuit voltage was measured with a Keithley 2400 source measure unit. Furthermore, the instrument was used as a variable load and the output voltage was measured to obtain the maximum power that the device could produce. Additionally, the Seebeck coefficient of an n-type leg was determined by measuring the voltage for different temperature gradients (between hot plate and room temperature) using a Keithley 2400 source measure unit.

Supporting Information

Supporting Information is available from the Wiley Online Library or from the author.

Acknowledgements

The authors gratefully acknowledge financial support from the Wallenberg Wood Science Center (WWSC). This project was in part performed at the Chalmers Materials Analysis Laboratory (CMAL). The authors thank Anders Mårtensson for his assistance with the SEM measurements.

Conflict of Interest

The authors declare no conflict of interest.

Data Availability Statement

The data that support the findings of this study are available from the corresponding author upon reasonable request.

Keywords

electrically conducting regenerated cellulose yarn, electronic textiles (e-textiles), organic thermoelectrics, poly(benzimidazobenzophenanthroline) (BBL), thermoelectric textile devices

Received: November 13, 2022
Revised: December 19, 2022
Published online:

[1] G. Chen, X. Xiao, X. Zhao, T. Tat, M. Bick, J. Chen, *Chem. Rev.* **2022**, *122*, 3259.
[2] K. Du, R. Lin, L. Yin, J. S. Ho, J. Wang, C. T. Lim, *iScience* **2022**, *25*, 104174.
[3] S. Takamatsu, T. Lonjaret, D. Crisp, J.-M. Badier, G. G. Malliaras, E. Ismailova, *Sci. Rep.* **2015**, *5*, 15003.
[4] S. Takamatsu, T. Lonjaret, E. Ismailova, A. Masuda, T. Itoh, G. G. Malliaras, *Adv. Mater.* **2016**, *28*, 4485.
[5] S. Sinha, R. Daniels, O. Yassin, M. Baczkowski, M. Tefferi, A. Deshmukh, Y. Cao, G. Sotzing, *Adv. Mater. Technol.* **2022**, *7*, 2100548.

[6] Z. Li, S. K. Sinha, G. M. Treich, Y. Wang, Q. Yang, A. A. Deshmukh, G. A. Sotzing, Y. Cao, *J. Mater. Chem. C* **2020**, *8*, 5662.
[7] J. Chen, Y. Huang, N. Zhang, H. Zou, R. Liu, C. Tao, X. Fan, Z. L. Wang, *Nat. Energy* **2016**, *1*, 16138.
[8] M. Hatamvand, E. Kamrani, M. Lira-Cantú, M. Madsen, B. R. Patil, P. Vivo, M. S. Mehmood, A. Numan, I. Ahmed, Y. Zhan, *Nano Energy* **2020**, *71*, 104609.
[9] N. Soin, T. H. Shah, S. C. Anand, J. Geng, W. Pornwannachai, P. Mandal, D. Reid, S. Sharma, R. L. Hadimani, D. V. Bayramol, E. Siores, *Energy Environ. Sci.* **2014**, *7*, 1670.
[10] A. Lund, K. Rundqvist, E. Nilsson, L. Yu, B. Hagström, C. Müller, *npj Flexible Electron.* **2018**, *2*, 9.
[11] X. Pu, L. Li, H. Song, C. Du, Z. Zhao, C. Jiang, G. Cao, W. Hu, Z. L. Wang, *Adv. Mater.* **2015**, *27*, 2472.
[12] J. Pope, C. Lekakou, *Smart Mater. Struct.* **2019**, *28*, 095006.
[13] T. Sun, B. Zhou, Q. Zheng, L. Wang, W. Jiang, G. J. Snyder, *Nat. Commun.* **2020**, *11*, 572.
[14] A. Lund, Y. Tian, S. Darabi, C. Müller, *J. Power Sources* **2020**, *480*, 228836.
[15] H. M. Elmoughni, A. K. Menon, R. M. W. Wolfe, S. K. Yee, *Adv. Mater. Technol.* **2019**, *4*, 1800708.
[16] S. J. Kim, J. H. We, B. J. Cho, *Energy Environ. Sci.* **2014**, *7*, 1959.
[17] L. K. Allison, T. L. Andrew, *Adv. Mater. Technol.* **2019**, *4*, 1800615.
[18] K. Kirihara, Q. Wei, M. Mukaida, T. Ishida, *Synth. Met.* **2017**, *225*, 41.
[19] J. A. Lee, A. E. Aliev, J. S. Bykova, M. J. de Andrade, D. Kim, H. J. Sim, X. Lepró, A. A. Zakhidov, J.-B. Lee, G. M. Spinks, S. Roth, S. J. Kim, R. H. Baughman, *Adv. Mater.* **2016**, *28*, 5038.
[20] A. Lund, N. M. van der Velden, N.-K. Persson, M. M. Hamedi, C. Müller, *Mater. Sci. Eng., R* **2018**, *126*, 1.
[21] J. Liu, G. Liu, J. Xu, C. Liu, W. Zhou, P. Liu, G. Nie, X. Duan, F. Jiang, *ACS Appl. Energy Mater.* **2020**, *3*, 6165.
[22] Y. Lin, J. Liu, X. Wang, J. Xu, P. Liu, G. Nie, C. Liu, F. Jiang, *Compos. Commun.* **2019**, *16*, 79.
[23] N. Komatsu, Y. Ichinose, O. S. Dewey, L. W. Taylor, M. A. Trafford, Y. Yomogida, G. Wehmeyer, M. Pasquali, K. Yanagi, J. Kono, *Nat. Commun.* **2021**, *12*, 4931.
[24] M. Ito, T. Koizumi, H. Kojima, T. Saito, M. Nakamura, *J. Mater. Chem. A* **2017**, *5*, 12068.
[25] J. Choi, Y. Jung, S. J. Yang, J. Y. Oh, J. Oh, K. Jo, J. G. Son, S. E. Moon, C. R. Park, H. Kim, *ACS Nano* **2017**, *11*, 7608.
[26] T. Bashir, M. Skrifvars, N.-K. Persson, *Polym. Adv. Technol.* **2011**, *22*, 2214.
[27] A. Lund, S. Darabi, S. Hultmark, J. D. Ryan, B. Andersson, A. Ström, C. Müller, *Adv. Mater. Technol.* **2018**, *3*, 1800251.
[28] X. Lan, T. Wang, C. Liu, P. Liu, J. Xu, X. Liu, Y. Du, F. Jiang, *Compos. Sci. Technol.* **2019**, *182*, 107767.
[29] Y. Zheng, Q. Zhang, W. Jin, Y. Jing, X. Chen, X. Han, Q. Bao, Y. Liu, X. Wang, S. Wang, Y. Qiu, C.-a. Di, K. Zhang, *J. Mater. Chem. A* **2020**, *8*, 2984.
[30] J. D. Ryan, A. Lund, A. I. Hofmann, R. Kroon, R. Sarabia-Riquelme, M. C. Weisenberger, C. Müller, *ACS Appl. Energy Mater.* **2018**, *1*, 2934.
[31] T. Zhang, K. Li, J. Zhang, M. Chen, Z. Wang, S. Ma, N. Zhang, L. Wei, *Nano Energy* **2017**, *41*, 35.
[32] T. Ding, K. H. Chan, Y. Zhou, X.-Q. Wang, Y. Cheng, T. Li, G. W. Ho, *Nat. Commun.* **2020**, *11*, 6006.
[33] J.-Y. Kim, J.-H. Mo, Y. H. Kang, S. Y. Cho, K.-S. Jang, *Nanoscale* **2018**, *10*, 19766.
[34] H. Sixta, A. Michud, L. Hauru, S. Asaadi, Y. Ma, A. W. T. King, I. Kilpeläinen, M. Hummel, *Nord. Pulp Pap. Res. J.* **2015**, *30*, 43.
[35] Y. Ma, M. Hummel, M. Määttänen, A. Särkilahti, A. Harlin, H. Sixta, *Green Chem.* **2016**, *18*, 858.
[36] C.-Y. Yang, M.-A. Stoeckel, T.-P. Ruoko, H.-Y. Wu, X. Liu, N. B. Kolhe, Z. Wu, Y. Puttisong, C. Musumeci, M. Massetti, H. Sun, K. Xu, D. Tu, W. M. Chen, H. Y. Woo, M. Fahlman, S. A. Jenekhe, M. Berggren, S. Fabiano, *Nat. Commun.* **2021**, *12*, 2354.
[37] S. Darabi, M. Hummel, S. Rantasalo, M. Rissanen, I. Öberg Månsson, H. Hilke, B. Hwang, M. Skrifvars, M. M. Hamedi, H. Sixta, A. Lund, C. Müller, *ACS Appl. Mater. Interfaces* **2020**, *12*, 56403.
[38] S. Asaadi, M. Hummel, P. Ahvenainen, M. Gubitosi, U. Olsson, H. Sixta, *Carbohydr. Polym.* **2018**, *181*, 893.